Extended Abstracts of the 2020 International Conference on Solid State Devices and Materials, VIRTUAL conference, 2020, pp83-84

Nanoscale Limits of Resistance Switching in Some Oxides and 2D Chalcogenide Materials

Eric Pop

Electrical Engineering, Materials Science & Engineering, and SystemX Alliance
Stanford University, Stanford, CA 94305, U.S.A. Contact: epop@stanford.edu

Reversible resistance switching in some chalcogenide compounds (like GeSbTe) and certain oxides (like VO_2) have been studied for more than half a century [1,2]. However, due to advances in nanofabrication, only in the last few years have devices based on these materials approached nanometer scale, near-atomic limits [3,4].

This talk will present recent highlights from our research on phase-change memory (PCM) materials, resistive random-access memory (RRAM) and insulator-metal transition (IMT) oxides. The results span from measurements of thermal and electrical properties of such devices and their interfaces, to understanding their fundamental size and energy limitations [5], at sub-10 nm dimensions whenever possible.

We find that energy-efficiency of PCM can be significantly improved by using two-dimensional (2D) materials and thermal insulators [6,7] (**Fig. 1**), and by reducing the programming pulse widths, to few nanoseconds. We use Raman thermometry and scanning thermal microscopy (SThM) to probe the temperature in functioning PCM devices [8,9], including those based on emerging 2D materials like $MoTe_2$ [10]. Applied to RRAM devices, SThM imaging reveals the formation of individual filaments [11] (**Fig. 2**). Simulations [5] and additional measurements [12] reveal that thermal and electrical contact resistance often dominate the behavior of such nanoscale memory.

Turning to IMT materials like VO_2, we use single-wall metallic carbon nanotubes (CNTs) as ultra-narrow (~1 nm) electrodes to probe the IMT at the nanoscale [4]. The CNT electrodes reduce the heated VO_2 volume to few-nanometer regions, enabling fast spiking oscillators for neuromorphic applications [13] (**Fig. 3**).

Taken together, these results probe the fundamental limitations of PCM, RRAM, and IMT technology, providing important insights for future energy-efficient designs.

References:

[1] S. Ovshinsky, *Phys. Rev. Lett.* 21, 1450 (1968)
[2] F.J. Morin, *Phys. Rev. Lett.* 3, 34 (1959)
[3] F. Xiong, A.D. Liao, D. Estrada, E. Pop, *Science* 332, 568 (2011)
[4] S.M. Bohaichuk et al., *ACS Nano*, 13, 11070 (2019)
[5] F. Xiong, E. Pop et al., *IEEE Intl. Electron Devices Meeting (IEDM)*, Dec 2016
[6] C. Ahn, S.W. Fong, et al., *Nano Letters* 15, 6809 (2015)
[7] C.M. Neumann, et al., *Appl. Phys. Lett.* 114, 082103 (2019)
[8] S.W. Fong, C.M. Neumann et al., *IEEE Trans. Electron Dev*. 64, 4496 (2017)
[9] E. Yalon, S. Deshmukh, et al., *Scientific Reports* 7, 15360 (2017)
[10] I.M. Datye, M. Muñoz Rojo, et al., *Nano Letters* 20, 1461 (2020)
[11] S. Deshmukh, M. Muñoz Rojo, et al., *IEEE Device Research Conference (DRC)*, Jun 2018
[12] S. Deshmukh, E. Yalon, et al., *IEEE Trans. Elec. Dev*. 66, 3816 (2019)
[13] S.M. Bohaichuk et al., *Nano Letters* 19, 6751 (2019)

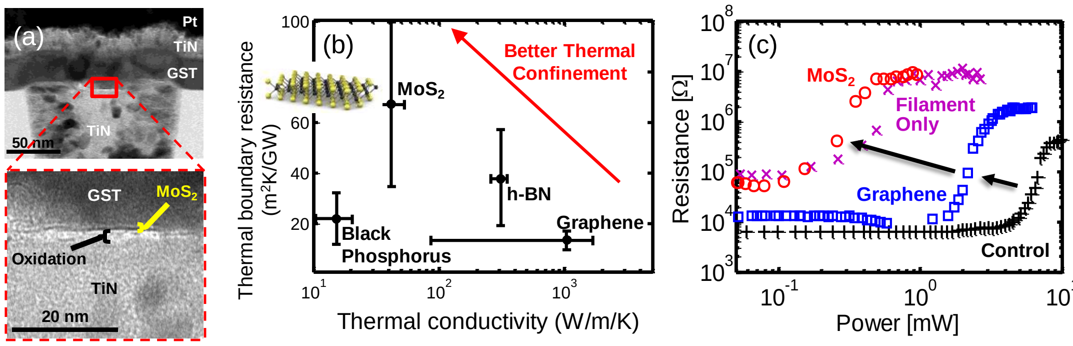

Fig. 1. PCM with 2D material thermal insulation layer [7]. (a) Cross-sectional transmission electron microscopy (TEM) image of the fabricated PCM device, with monolayer MoS_2 at the $Ge_2Sb_2Te_5$ (GST) interface with the bottom electrode. (b) Trend of thermal conductivity and thermal boundary resistance (TBR) among several considered 2D materials [6,7]. (c) Electrical measurements of PCM cells with MoS_2 and graphene thermal insulation layer, compared to control device [7].

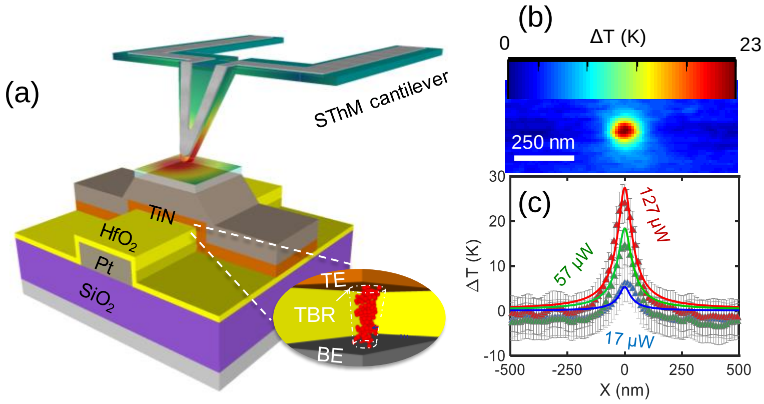

Fig. 2. (a) Schematic of scanning thermal microscopy (SThM) measurements of functioning RRAM device based on HfO_2 [11]. (b) Top-side SThM imaging of nanoscale filamentary hot spot, and (c) estimated temperature rise recorded by SThM. Note that SThM measures the top electrode temperature, and simulations are used to deduce the filamentary temperature within the RRAM (>1200 K).

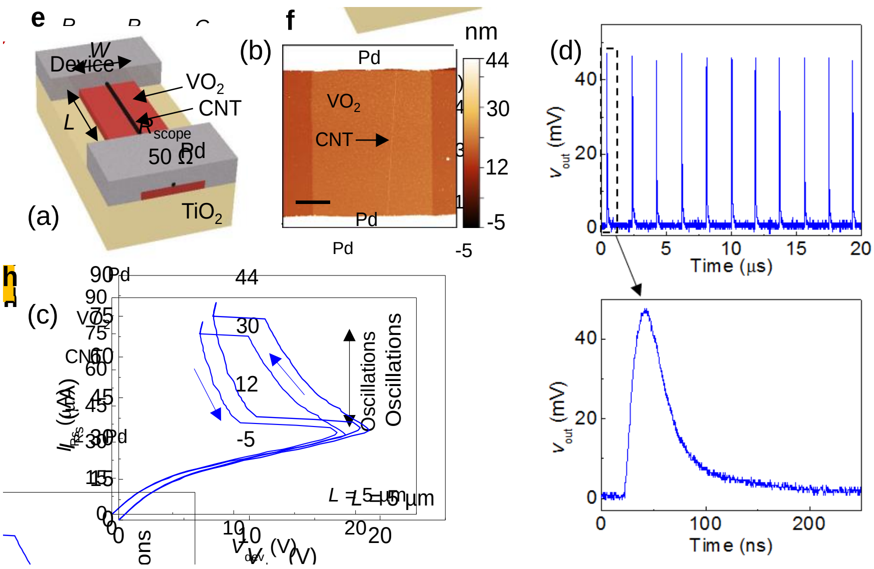

Fig. 3. (a) Schematic and (b) atomic force microscopy (AFM) image of VO_2 device with CNT heater electrode. (c) Measured quasi-static current-voltage behavior of such a device, causing oscillations when biased in the negative differential resistance (NDR) region. (d) Periodic voltage spiking of a device driven by a 60 μA DC current, measured across the 50 Ω load of the oscilloscope.